Proc. Natl. Acad. Sci. USA
Vol. 82, pp. 7791–7795, November 1985
Physiological Sciences

Single anion-selective channels in basolateral membrane of a mammalian tight epithelium

(patch clamp/chloride conductance/anion channel/epithelial transport)

J. W. HANRAHAN, W. P. ALLES, AND S. A. LEWIS

Department of Physiology, Yale University School of Medicine, New Haven, CT 06510

Communicated by Gerhard Giebisch, July 15, 1985

ABSTRACT **Basolateral membrane chloride permeability of surface cells from rabbit urinary bladder epithelium was studied using the patch-clamp technique. Two types of anion-selective channel were observed. One channel type showed inward rectification and had a conductance of 64 pS at −50 mV when bathed symmetrically by saline solution containing 150 mM chloride; the other resembled high-conductance voltage-dependent anion channels (VDACs). Both channels had the selectivity sequence $Cl^- \approx Br^- \approx I^- \approx SCN^- \approx NO_3^- > F^- >$ acetate > gluconate > $Na^+ \approx K^+$ and were sensitive to the anion exchange inhibitor 4,4′-diisothiocyanostilbene-2,2′-disulfonic acid. Basolateral chloride conductance in urinary bladder is apparently due to the 64 pS anion channel, which is active at physiological potentials. Imperfect selectivity of this channel against cations might also account for the low, but finite, sodium permeability of the basolateral membrane.**

Membrane chloride conductance is an essential feature of cellular models for chloride transport across the cornea (1), trachea (2), and thick ascending limb of Henle's loop (3) and is thought to be an important regulatory site for fluid secretion and cell-volume regulation in some cells (4–7). However, unlike sodium and potassium channels, which have been characterized using fluctuation analysis (8, 9), little is known regarding anion permeability in most epithelia, and its constituent ion channels have not been identified (10). The rabbit urinary bladder is a model tight epithelium which has very high basolateral chloride permeability (11). We used the patch-clamp technique (12) to study this chloride conductance at the single-channel level.

MATERIALS AND METHODS

Epithelial cells were scraped from the luminal surface of rabbit urinary bladders and exposed to high-purity collagenase (100 units/ml; Worthington or Sigma) dissolved in a 1:1 mixture of medium 199 and Ham's nutrient mixture F-12 (GIBCO) at room temperature (22 ± 2°C). The epithelium of mammalian urinary bladder is transitional, consisting of large (≈70 μm diameter), flattened surface cells and two lower layers of much smaller (10 μm), cuboidal cells. Brief exposure to collagenase left a few intermediate cells attached to those from the surface layer, enabling us to identify the basolateral membrane during experiments. When obtaining seals, the patch pipette was placed against the surface cell's basolateral membrane next to the attached intermediate cells. The basolateral origin of patches was often confirmed by the presence of both anion- and potassium-selective channels because the apical membrane of this tissue does not exhibit potassium- or anion-selective conductances (13). Single-channel currents were recorded by use of pipettes made from borosilicate glass tubing (Boralex, Rochester Scientific, NY) that had been pulled and coated by standard methods (12). Seal resistances were typically 5–60 GΩ.

Currents were recorded on FM tape, low-pass filtered at 800 Hz during playback using an 8-pole Bessel filter (902 LPF, Frequency Devices, Haverhill, MA) and digitized at 2 or 4 KHz to give records containing 16,384 points. Each digitized record was displayed in blocks of 2048 points for inspection of events, and the mean baseline (leakage) current and its variance were calculated between two points that were set using a cursor. Data were normalized to the baseline, sometimes edited to remove transients and invalid events, and then analyzed to produce a histogram of current amplitudes. Open- and closed-time histograms were calculated using a threshold setting of one-half the open-channel current, as deduced from the amplitude histogram. Test pulses of various durations were used to determine the minimal duration that could be detected under experimental conditions. Events lasting <2 msec but >400 μsec became distorted in shape but still crossed the 50% threshold and were counted. Nevertheless, the first bin in closed-time histograms (<500 μsec) was not used when fitting exponentials, and time constants less than about 2 msec should be regarded as first estimates until a wider-pass band can be used. In both open- and closed-time histograms, the actual number of events in each bin was plotted and fitted rather than the cumulative distribution. To obtain power-density spectra, the data were low-pass filtered at 900 Hz with a 20-pole Cauer elliptic filter (LP120, Unigon, Mount Vernon, NY), digitized at 2 kHz, and read as 16 consecutive records of 2048 points each. Thirty-two spectra were obtained from overlapped data blocks by fast Fourier transform, averaged to yield final spectra, and fitted as the sum of linear and Lorentzian-type functions.

The pipette solution was 150 mM KCl (or NaCl)/10 mM Hepes, pH 7.2/80 μM EGTA. The initial, extracellular solution was 140 mM NaCl/6 mM KCl/2 mM $MgCl_2$/2 mM $CaCl_2$/20 mM Hepes pH 7.2. To determine selectivity among anions, patches were excised and the bath was perfused with a solution that was identical to that in the pipette except that chloride was replaced with a different anion. Liquid junctions were kept biionic, and those arising at the reference agar bridge were measured relative to a flowing 3 M KCl junction as follows. First, a 150 mM KCl solution was placed in the bath and a 150 mM KCl/4% agar bridge was connected to the bath reference electrode (Ag/AgCl). The tip of a patch pipette (containing another Ag/AgCl electrode) then was filled with 3 M KCl and immersed in the bath, and current flowing through the pipette was clamped at zero while the bath solution was replaced by other salts of potassium. The voltage deflections caused by substituting other anions for chloride agreed with those expected from their free-solution mobilities and were used to correct measured reversal poten-

The publication costs of this article were defrayed in part by page charge payment. This article must therefore be hereby marked "*advertisement*" in accordance with 18 U.S.C. §1734 solely to indicate this fact.

Abbreviations: DIDS, 4,4′-diisothiocyanostilbene-2,2′-disulfonic acid; VDAC, voltage-dependent anion channel.

tials. Experiments were performed at room temperature (≈22°C).

RESULTS

Conductance and Selectivity

Low-Conductance Anion Channel (g_{64}). Fig. 1*A* shows the current recorded from an inside-out patch excised from the basolateral membrane of a surface cell and held at −50 mV, approximately the normal potential *in situ* (11). This particular recording was obtained when the patch was bathed symmetrically by 150 mM KCl, but similar results were obtained when the solution on either (or both) sides of the membrane contained NaCl. Single-channel currents displayed inward rectification (Fig. 1*B*), and their open-channel current/voltage (I/V) relationship yielded a mean slope conductance in six patches of 64.0 ± 4.7 pS between −40 and −60 mV. Fig. 1*B* also shows the I/V relationship after substitution of fluoride for chloride. With a 5:1 KCl gradient, single-channel currents changed sign at approximately −20 to −35 mV, from which we calculated a value for P_{K^+}/P_{Cl^-} (permeability ratio) of 0.043 ± 0.016 (mean ± SEM, n = 6 patches), using the constant field equation (14, 15). We measured similar reversal potentials under biionic conditions and measured nearly identical slope conductances between −40 and −60 mV when currents were carried by anions from the bath. These observations indicated that this channel is equally permeable to Cl^-, Br^-, I^- NO_3^-, and SCN^-, within measurement error ($P > 0.2$, n = 3). However, we calculated P_{F^-}/P_{Cl^-} = 0.479 (n = 1), $P_{acetate}/P_{Cl^-}$ = 0.310 ± 0.036 (n = 3), and $P_{gluconate}/P_{Cl^-}$ = 0.07 ± 0.040 (n = 3). Bicarbonate ions also permeate, but less well than chloride ions.

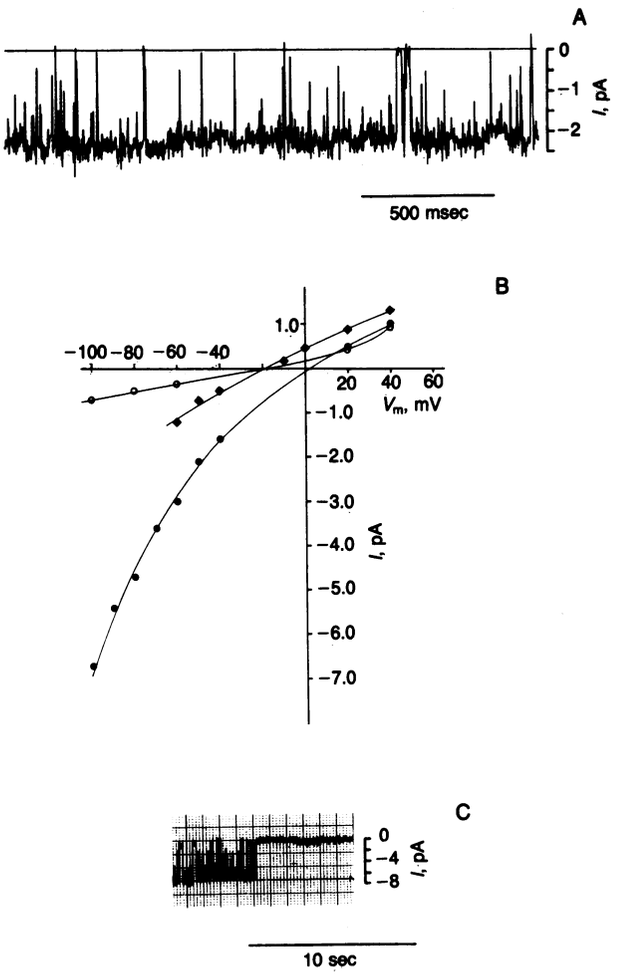

FIG. 1. Low-conductance anion channel (g_{64}) in basolateral membrane patch excised from rabbit urinary bladder. (*A*) Recording from excised, inside-out patch bathed on both sides with solution containing 150 mM KCl and with membrane potential (V_m) held at −50 mV. (*B*) Single-channel current/voltage (I/V) relationship observed in symmetrical KCl (●) with a 5:1 KCl gradient (○) and after replacement of chloride in the bath with fluoride (◆). (*C*) Deactivation of g_{64}; trace begins immediately after stepping V_m from 0 mV to −100 mV.

Discrimination between fluoride and other halides having lower free energies of hydration suggests that permeating anions interact with a site having low field strength, whereas acetate and gluconate are presumably distinguished by size. Importantly, g_{64} was often seen when we recorded in the cell-attached mode, indicating that it normally contributes to membrane conductance. The number of anion channels per patch ranged from zero to six. The overall probability of observing an anion channel after obtaining a gigaohm seal was about 0.3, however, there was day-to-day variability in the number of channels obtained even when care was taken to keep all experimental conditions constant. The cause of this variability has not been determined.

High-Conductance Anion Channel (g_{362}). A much larger unit conductance (362.3 ± 11.1 pS; mean ± SEM, 9 patches), referred to here as the high-conductance channel or g_{362}, was observed in excised patches after a variable delay of 30 sec to several minutes (Fig. 2*A*). This channel usually did not appear until large (*ca.* ±50 mV) voltage steps were applied, but once evoked, it would remain spontaneously active at potentials between +20 and −20 mV. We assessed the selectivity of g_{362} under the same biionic conditions used to study g_{64} (Fig. 1*B*). As before, the reversal potential with a 5:1 KCl gradient present was approximately −35 mV, yielding P_{K^+}/P_{Cl^-} = 0.059 ± 0.01 (n = 10 patches). Moreover, replacing bath Cl^- with NO_3^-, SCN^-, I^-, or Br^- had no significant effect on the reversal potential ($P > 0.2$). We estimated P_{F^-}/P_{Cl^-} = 0.57 ± 0.05 (n = 3), $P_{acetate}/P_{Cl^-}$ = 0.30 ± 0.03 (n = 3), and $P_{gluconate}/P_{Cl^-}$ = 0.07 ± 0.01 (n = 4). In summary, the selectivities of g_{64} and g_{362} were identical for all ions tested, providing evidence that the sites (i.e., filters) responsible for selectivity in both channels might have structural similarities despite their very different conductances.

Kinetics

The low-conductance anion channel (g_{64}) remained active indefinitely at normal potentials (*ca.* −50 mV) but became quiescent after several seconds when the membrane potential (V_m) was made more negative than −80 mV (Fig. 1*C*). This deactivation occurred in <1 sec at more hyperpolarized potentials, but channel activity was restored when the membrane potential was returned to a value more positive than about −80 mV. In contrast, g_{362} inactivated at the normal membrane potential of −50 mV. A stimulus, such as stepping V_m to the opposite polarity, was required to cause g_{362} to reopen, although it would rapidly inactivate again. We noticed that g_{362} usually inactivated outside the range ±20 mV and that this occurred much more rapidly at large positive potentials than at large negative ones, which sometimes required >4 min. Such voltage-dependent behavior is of uncertain physiological significance (see below) but suggests that this channel would not normally be active *in situ*. Finally, in contrast to the single conductance level of g_{64}, the high-conductance channel displayed numerous subconductance states. These transitions were rectangular, clearly resolved, and often lasted for >10 msec. One substate flickered to the fully open state and is shown with low time resolution in Fig. 2*C*.

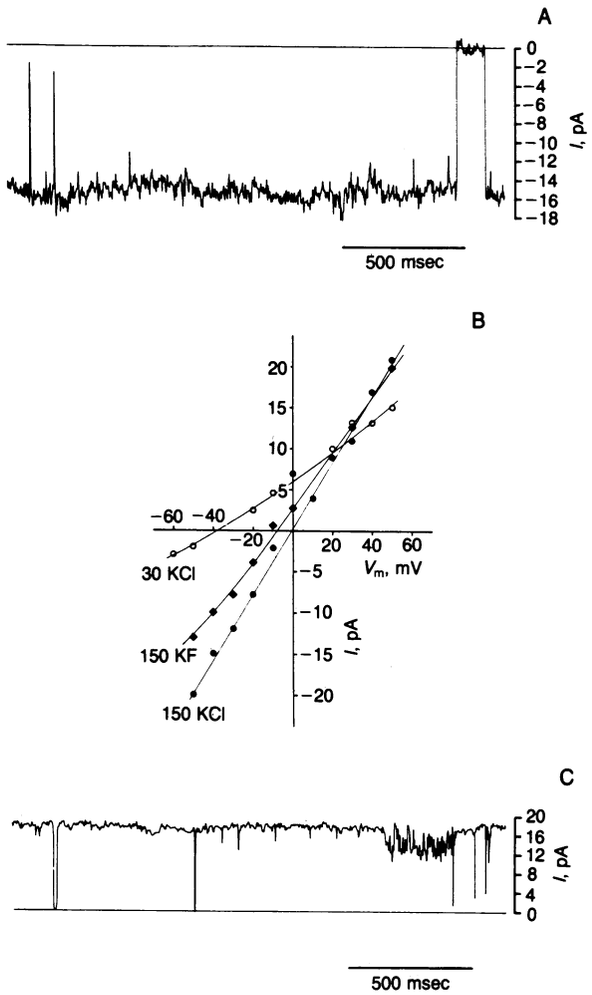

FIG. 2. High-conductance anion channel (g_{362}). (*A*) Recording made under same experimental conditions as in Fig. 1. (*B*) Single-channel I/V relationship (see legend of Fig. 1 for conditions). (*C*) g_{362} shown at V_m = +50 mV to illustrate the presence of conductance substates. These substates showed the same reversal potentials as the main open state and were abolished at negative potentials by replacing chloride on the cytoplasmic side of the membrane with gluconate.

We studied the kinetics of g_{64} in more detail because it was observed in cell-attached patches and because it remained active indefinitely at normal membrane potentials, whereas g_{362} did not. Fluctuation analysis of the current records from g_{64} yielded spectra that could be fitted with two Lorentzian-type components, one having a corner frequency of about 30 Hz ($f_{c,1}$), and another, high-frequency component between 160 and 220 Hz ($f_{c,2}$), suggestive of at least three kinetic states (Fig. 3*A*). Fig. 3*B* shows an amplitude histogram calculated as described in *Materials and Methods*. Histogram peaks, corresponding to patch current when the channel was open or closed, appeared normally distributed; this was especially clear at large holding voltages, when the peaks were widely separated, and suggests that most transitions were not attenuated by our filter. The distribution of channel open times was fitted reasonably well by a single exponential function (Fig. 3*C*), whereas two exponentials were required to fit histograms of closed durations (Fig. 3*D*). Also, data from power spectra compared favorably with the mean open and closed times obtained by time-domain analysis (see ref. 16). By use of the mean open time ($\bar{t}_o$ = 28.3 ± 2.34 msec; 19 analyses of 6 patches), the longer of the two mean closed times (which could be clearly resolved; $\bar{t}_c$ = 6.7 ± 0.49 msec), and the equation $1/\tau = 2\pi f_c$, it was possible to estimate the lower corner frequency: $f_{c,1} = (\bar{t}_o + \bar{t}_c)/2\pi\bar{t}_o\bar{t}_c$. The predicted (30.3 ± 2.0 Hz; 37 single-channel analyses, 6 patches) and experimental values (32.9 ± 3.9 Hz; 24 spectra, 6 patches) agreed, as expected when the two Lorentzian components in a power spectrum have widely separated corner frequencies (17). Also, the plateau values (S_o) calculated under these conditions by using $\bar{t}_o$, the open-state probability (P_o), and the equation $S_o = I^2P_o/\bar{t}_o\pi^2f_c^2$ were nearly identical to those measured (see Fig. 3*B*), confirming the presence of a single active channel in each patch. No consistent differences in gating were observed when the current was carried by anions other than chloride.

A kinetic scheme for g_{64} will be proposed in a later paper; however, from the two Lorentzian components in the power spectra and the double exponentials in the closed-time histogram, several kinetic states can be inferred. They would correspond to long openings (≈25 msec) and to brief- and long-lived closures (<1 msec and ≈6 msec, respectively). The sum of the closing rate constants is thus about 40 sec^{-1}.

At potentials between −20 and −100 mV, the probability of g_{64} being open while active (i.e., during fast open–closed transitions, P_o; Fig. 4) did not depend on voltage and was 0.92 ± 0.01 (42 analyses of 6 patches). No change was observed in the mean duration of open or closed events at potentials where deactivation occurred, implying the presence of a third, deactivated state in addition to the two closed states mentioned above in connection with closed-time histograms and power spectra. Rates of entering and leaving the deactivated state are apparently voltage-dependent, with the former rate constant being negligible between 0 mV and −80 mV but ≈0.5 sec^{-1} at −90 mV. We noticed that the fast open–closed transitions of g_{64} became even more rapid at positive (nonphysiological) potentials, and P_o declined (Fig. 4).

Raising the concentration of free calcium from <10 nM to >1 mM on either side of the membrane had no detectable effects on the gating of g_{64} or g_{362}.

Effect of 4,4′-Diisothiocyanostilbene-2,2′-Disulfonic Acid (DIDS). Inhibition of chloride fluxes by DIDS has sometimes been used as evidence for anion exchange; however, this is apparently not a useful criterion in distinguishing exchange from conductive mechanisms in rabbit bladder because both anion channels in this study were sensitive to DIDS (0.1 mM) when applied to the internal membrane surface, and g_{64} was irreversibly inhibited by external DIDS at the same concentration after 2–3 sec.

DISCUSSION

To our knowledge, the low-conductance anion channel (g_{64}) described here has not been detected by use of the patch-clamp technique, although a rectifying chloride channel having similar conductance has been incorporated into planar lipid bilayers from cardiac sarcolemma vesicles (18). The cardiac channel shows somewhat different kinetics, opening in bursts that have a time scale of seconds at −50 mV; its selectivity between different anions was not reported.

Except for somewhat higher selectivity, the high-conductance anion channel g_{362} is strikingly similar to voltage-dependent anion channels (VDACs) from mitochondrial outer membrane (19, 20) and to anion channels recently described in primary cultures of rat muscle, rabbit urinary bladder epithelium, and rabbit glial cells and in several continuous cell lines (embryonic carcinoma, A6, and MDCK cells) (21–27). Nearly all plasmalemma VDACs reported to date have been from cultured cells, and all eventually become inactive at potentials outside the range ±20 mV; hence, their physiological function, if any, is a mystery. A developmental role might explain their widespread distribution in a variety of cultured cells; however, the VDACs described in this study were from uncultured, fully differentiated cells from

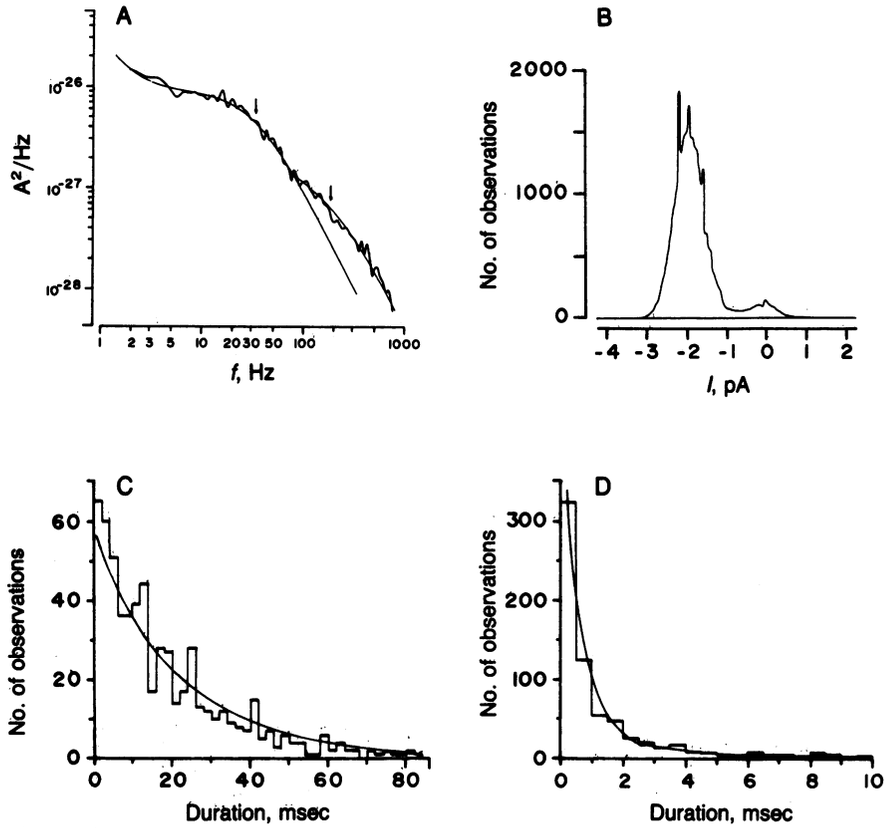

FIG. 3. Kinetics of the low-conductance anion channel g_{64}. (*A*) Power spectrum of current flowing through an inside-out patch containing a single anion channel. The membrane was bathed symmetrically with 150 mM KCl solution and held at −60 mV. The smooth lines indicate two Lorentzian-type components, suggesting at least three states. The plateau values ($S_{o,1}$ and $S_{o,2}$) are (0.90 ± 0.011) × 10^{-26} and (0.11 ± 0.002) × 10^{-26} A^2·sec (best-fit ± SD), respectively. The lower plateau value agrees well with predictions based on single-channel current, open-state probability, and mean open time (1.4 × 10^{-26} A^2·sec, see text). Corner frequencies of the two components are 33.7 ± 0.38 Hz and 187.9 ± 2.46 Hz (best fit ± SD) and are indicated by arrows. (*B*) Histogram of current amplitude at −50 mV from a patch bathed symmetrically with 150 mM KCl solution: single-channel current = 1.82 pA [mean; variance (after subtraction of baseline noise) = 0.172 pA^2]; open-state probability P_o = 0.9197; 30,719 observations. (*C*) Duration histogram of open-channel events ($\bar{\tau}_o$ = 21.9 msec; r^2 = 0.87). (*D*) Duration histogram of closed-channel events ($\bar{\tau}_c$ = 0.9 msec and 5.2 msec; r^2 = 0.88 and 0.74, respectively).

adult rabbits, and similar channels have been reported in peritoneal macrophages (28), which are also presumably differentiated. We usually observed low-conductance anion channels in excised patches immediately before VDACs became active. This finding, combined with their identical selectivities and the fact that both channels are DIDS- and voltage-sensitive, hints that the plasmalemma VDAC in rabbit urinary bladder might be a relative of the 64 pS anion channel or perhaps a breakdown product of it.

Regardless of this possible relationship, g_{64} is active at normal membrane potentials and so would be responsible for basolateral membrane chloride conductance in the rabbit urinary bladder. Cation selectivity of this channel (0.043) is remarkably similar to earlier macroscopic estimates of P_{Na^+}/P_{Cl^-} for the basolateral membrane (0.038), so g_{64} may also account for basolateral permeability to sodium ions in this epithelium (11).

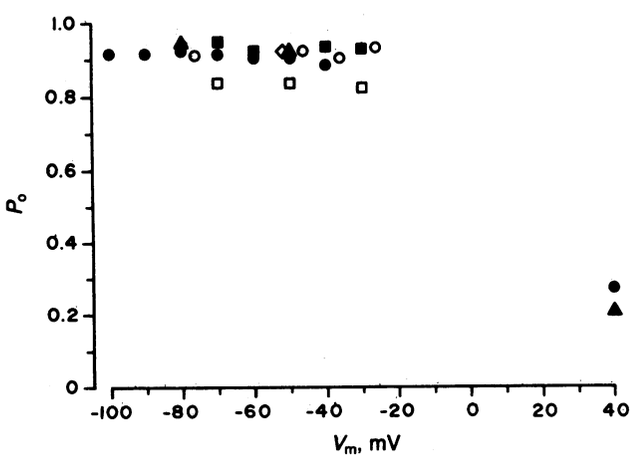

FIG. 4. Relationship between the probability of g_{64} being in the open state while active (P_o) and membrane voltage. P_o was calculated only for periods of rapid transitions; g_{64} eventually deactivated at potentials more negative than −80 mV. Symbols represent six different inside-out patches. Each patch contained one functional channel and was bathed symmetrically with 150 mM KCl solution.

The voltage dependence of g_{64} (deactivation at hyperpolarized potentials) and the channel's weak selectivity among anions are qualitatively similar to the characteristics of chloride conductance in amphibian skin, which have been studied by transepithelial voltage clamping (29, 30). The chloride conductance of toad skin characterized by Larsen and coworkers (e.g., ref. 31) is thought to reside in the apical membrane of the mitochondria-rich cells and is activated when the transepithelial potential is clamped outside-negative; i.e., when the apical membrane would be depolarized. If the intracellular potential in short-circuited toad skin is −70 to −100 mV as it is in the frog skin (32), the voltage dependent activation of chloride conductance could be accounted for by channels resembling g_{64}. There is evidence that the basolateral membrane of frog skin has a similar anion pathway that is sensitive to membrane voltage and cell volume (33). Further studies are needed to establish whether g_{64} is responsible for high basolateral chloride conductance in other epithelia, notably the thick ascending limb of Henle's loop (3) and collecting duct (34, 35), and whether it is present in membranes of such diverse tissues as cornea (1), insect hindgut (36), trachea (2), and *Necturus* gallbladder (37), where chloride conductance is known to be strongly modulated.

We thank Drs. B. P. Bean, F. J. Chlapowski, and M. C. Nowycky for their help during the initial stages of this work and Dr. R. W. Aldrich for comments on the manuscript. This work was supported by fellowships from the Natural Sciences and Engineering Research Council and Medical Research Council (Canada) to J.W.H. and by Grant AM33243 to S.A.L. from the National Institutes of Health.

1. Klyce, S. D. & Wong, R. K. S. (1977) *J. Physiol. (London)* **266,** 777–799.
2. Welsh, M. J., Smith, P. L. & Frizzell, R. A. (1982) *J. Membr. Biol.* **70,** 227–238.
3. Greger, R. & Schlatter, E. (1983) *Pflügers Archiv.* **396,** 325–334.

4. Grinstein, S., Clarke, C. A., Dupre, A. & Rothstein, A. (1982) *J. Gen. Physiol.* **80,** 801–823.
5. Ferreira, K. T. G. & Ferreira, H. G. (1981) *Biochim. Biophys. Acta* **646,** 193–202.
6. Ussing, H. H. (1982) *Acta Physiol. Scand.* **114,** 363–369.
7. Lewis, S. A., Butt, A. G., Bowler, M. J., Leader, J. P. & Macknight, A. D. C. (1985) *J. Membr. Biol.* **83,** 119–137.
8. Lindemann, B. & Van Driessche, W. (1977) *Science* **195,** 292–294.
9. Van Driessche, W. & Gögelein, H. (1978) *Nature (London)* **275,** 665–667.
10. Lewis, S. A., Hanrahan, J. W. & Van Driessche, W. (1984) in *Current Topics in Membranes and Transport*, ed. Stein, W. D. (Academic, New York), Vol. 21, pp. 253–293.
11. Lewis, S. A., Wills, N. K. & Eaton, D. C. (1978) *J. Membr. Biol.* **41,** 117–148.
12. Hamill, O. P., Marty, A., Neher, E., Sakmann, B. & Sigworth, F. J. (1981) *Pflügers Archiv.* **391,** 85–100.
13. Lewis, S. A., Ifshin, M. S., Loo, D. D. F. & Diamond, J. M. (1984) *J. Membr. Biol.* **80,** 135–151.
14. Goldman, D. E. (1943) *J. Gen. Physiol.* **27,** 37–60.
15. Hodgkin, A. L. & Katz, B. (1947) *J. Physiol. (London)* **108,** 37–60.
16. Colquhoun, D. & Hawkes, A. G. (1977) *Proc. R. Soc. London Ser. B* **199,** 231–262.
17. Lindemann, B. & Van Driessche, W. (1978) in *Membrane Transport Processes*, ed. Hoffman, J. F. (Raven, New York), Vol. 1, pp. 155–178.
18. Coronado, R. & Latorre, R. (1982) *Nature (London)* **298,** 849–852.
19. Schein, S. J., Colombini, M. & Finkelstein, A. (1979) *J. Membr. Biol.* **30,** 99–120.
20. Colombini, M. (1979) *Nature (London)* **279,** 643–645.
21. Blatz, A. L. & Magleby, K. L. (1983) *Biophys. J.* **43,** 237–241.
22. Hanrahan, J. W., Alles, W. P. & Lewis, S. A. (1984) *Biophys. J.* **45,** 300A (abstr.).
23. Gray, P. T. A., Bevan, S. & Ritchie, J. M. (1984) *Proc. R. Soc. London Ser. B* **221,** 395–409.
24. Simmoneau, M. (1984) *Biophys. J.* **45,** 308A (abstr.).
25. Nelson, D. J., Tang, J. M. & Palmer, L. G. (1984) *J. Membr. Biol.* **80,** 81–89.
26. Hunter, M., Cohen, B. J., Forrest, J. & Giebisch, G. (1984) *Fed. Proc. Fed. Am. Soc. Exp. Biol.* **43,** 302 (abstr.).
27. Kolb, H. A., Brown, C. D. A. & Murer, H. (1985) *Pflügers Archiv.* **403,** 262–265.
28. Schwarze, W. & Kolb, H. A. (1984) *Pflügers Archiv.* **402,** 281–291.
29. Larsen, E. H. & Kristensen, P. (1978) *Acta Physiol. Scand.* **102,** 1–21.
30. Kristensen, P. (1982) in *Chloride Transport in Biological Membranes*, ed. Zadunaisky, J. A. (Academic, New York), pp. 319–332.
31. Larsen, E. H. & Rasmussen, B. E. (1982) *Philos. Trans. R. Soc. London Ser. B* **299,** 413–434.
32. Nagel, W. (1976) *Pflügers Archiv.* **365,** 135–143.
33. Ussing, H. H. (1985) *Pflügers Archiv.*, in press.
34. Sansom, S. C., Weinman, E. J. & O'Neil, R. G. (1984) *Am. J. Physiol.* **247,** F291–F302.
35. Koeppen, B. M. (1985) *Am. J. Physiol.* **248,** F500–F506.
36. Hanrahan, J. W. & Phillips, J. E. (1984) *J. Membr. Biol.* **80,** 27–47.
37. Petersen, K.-U. & Reuss, L. (1983) *J. Gen. Physiol.* **81,** 705–729.